International Journal of Mathematical, Engineering and Management Sciences
Vol. 10, No. 5, 1324-1350, 2025
https://doi.org/10.33889/IJMEMS.2025.10.5.063

Ram Arti Publishers

A Distributed Privacy Preserved Federated Learning Approach for Revolutionizing Pneumonia Detection in Isolated Heterogenous Data Silos

Shagun Sharma
Chitkara University Institute of Engineering and Technology,
Chitkara University, Punjab, India.
&
School of Computing Science & Engineering,
VIT Bhopal University, Sehore, Bhopal, Madhya Pradesh, India.
E-mail: shagunsharma7098@gmail.com, shagun.sharma@chitkara.edu.in

Kalpna Guleria
Chitkara University Institute of Engineering and Technology,
Chitkara University, Punjab, India.
Corresponding author: guleria.kalpna@gmail.com, kalpna@chitkara.edu.in

(Received on February 4, 2025; Revised on April 15, 2025; Accepted on April 29, 2025)

Abstract
Pneumonia is a respiratory lung contamination that ranges in severity from mild to lethal outcomes. The analysis of tomographic images is the most significant method of pneumonia detection. The image analysis requires expertise and proficiency to diagnose the disease correctly. The medical reports with multiple diseases have overlapping symptoms, which may lead to misdiagnosis and deferred identification. The misdiagnosis results in increased healthcare costs, worsened medical conditions, and legal implications. Centralized deep learning enhances the feature extraction process and optimally improves the prediction outcomes; however, these models have data privacy concerns due to centralized storage systems. The healthcare departments follow the Health Insurance Portability and Accountability Act. (HIPAA) to maintain the retaining of patient data and improve the portability and continuity of health insurance coverage. In the proposed work, federated learning has been utilized to enhance data privacy and deal with imbalanced and diverse data silos. This distributed privacy-preserved model has been employed with a pooled dataset curated from multiple sources in a 5-client architecture. The model was implemented with the FedAVG aggregation technique in independent and identically distributed (IID) and non-IID data distributions. The outcomes of the model exhibit 87.62% accuracy with IID and 86.15% accuracy with non-IID distributions. The comparison of these outcomes with the existing studies shows that the proposed model outperforms by exhibiting better performance and resulting in the minimum loss of 0.4041 and 0.4139 with IID and non-IID distributions, respectively.

Keywords- Deep learning, InceptionV3, Distributed architecture, Federated learning, Pneumonia detection, Centralized learning.

1. Introduction

In 2019, the number of Covid-19 cases started to increase, resulting in a global health crisis and widespread transmission, hence WHO declaring it as a pandemic in March 2020 (Kafadar et al., 2022). It caused a rapid increase in mortality rates due to the unavailability of vaccines and medications. This pandemic directly impacted the patient care system and economic growth that limited medical resources and healthcare equipment's worldwide (Holt et al., 2020). The sudden surge of Covid-19 cases and immediate shutdowns led to a decrease in the available healthcare assets and medicine supplies. Covid-19 affects the respiratory system and results in reducing surfactant secretion (Alipoor et al., 2020). The decrease in secretion causes the alveoli to collapse, resulting in pneumonia. In the past 20 years, the mortality cases caused by pediatric pneumonia have significantly decreased (Kanwal et al., 2024). However, these cases started to increase during the pandemic, when the available healthcare resources were insufficient for the treatment of Covid-19. Pneumonia is respiratory lung contamination caused by bacteria and viruses and ranges from mild to

lethal outcomes (Adjei-Mensah et al., 2024). The advancement in pneumonia stages may affect other organs, such as the nervous system, heart, and lungs, along with blood vessels (Hatmi, 2021). The identification of pneumonia is challenging to the lower income countries due to the complex structure of the disease (Kundu et al., 2021). The other problem associated with this disease is its misdiagnosis due to the similar kinds of symptoms in tuberculosis, Covid-19, and lung cancer. As per the WHO report, pneumonia affects people over the age of 65 and patients with a weakened immune system the most (Pneumonia, n.d.). There are various other kinds of respiratory diseases, such as silicosis, chronic bronchitis, cystic fibrosis, asthma, lung cancer, and tuberculosis. The statistics presented in Goyal & Singh (2023), show that lung cancer has affected 8 million people to date; however, this patient count is less if compared to the 15-month cases of Covid-19 and pneumonia. Respiratory infections and diseases are detected using the tomography imaging process, specifically with X-ray scans; however, it requires expertise and proficiency to correctly diagnose the disease. Patients with multiple diseases may have overlapping symptoms in their reports, which creates complexity in accurately diagnosing the associated disease, and the obliviousness of the medical imaging process leads to misdiagnosis of the disease. The misdiagnosis of the disease may result in worse medical conditions, increased healthcare costs, psychological impact, and legal implications, along with lethal results. There are various existing studies that have used different kinds of artificial intelligence (AI) tools on medical images to accurately identify diseases. The deep learning (DL) models are also used for Alzheimer's, Parkinson's, pneumonia, cancer, and Covid-19 disease detection (Hariri & Avşar, 2023; Kafadar et al., 2022; Kundu et al., 2021; Prakash et al., 2023b; Prakash et al., 2023c; Rahimzadeh & Attar, 2020). These models are highly efficient and optimal for providing improved performance of disease detection by performing proficient image processing and feature extraction. The Xception, InceptionV3, VGG16, VGG19, ResNet50, CNN, and ensemble models have been used by various researchers to predict pneumonia from lung CXRs (Alyasseri et al., 2022; Gulati et al., 2022; Hasan et al., 2021; Ieracitano et al., 2022; Jaiswal et al., 2019; Prakash et al., 2023a; Rehman et al., 2022). These models have hierarchical feature learning, robustness to variance, higher scalability, and capability due to the handling of millions of parameters to capture the image data with vast complexities. These models are trained with the centralized learning process, where the data processing and computational tasks are performed within the central server using the vast volume of the data. DL presents various efficient approaches for optimally analyzing the images, while it also poses significant challenges such as scalability issues, data privacy concerns, and high time complexity due to transferring the data to the centralized location. Hence, federated learning (FL) was introduced by Google in 2016 to enhance data privacy, improve scalability, increase bandwidth, and deal with diverse datasets (Khan & Alam, 2021; Nair et al., 2022). The base models used in the distributed FL are DL models. This framework contains various clients and a single server allowing local training at the client location by sending the initial model from the server to each client (Wahab et al., 2023). The clients further perform local training with the model and send the model updates to the server instead of sending the data (Zhang et al., 2024). The server then aggregates the local updates by using the averaging technique and creates a global model to perform global training. Though the communication overhead in the FL is higher while, it ensures that the patient's data remains private and unshared with the other clients and servers participating in the architecture (Darzi et al., 2024; Hoyos et al., 2023; Wahab et al., 2023).

In the proposed work, the traditional DL-based InceptionV3 and distributed FL-based InceptionV3 model have been proposed for pneumonia detection. The FL was applied with two different distributions, namely IID and non-uniform data distribution, and the existence of pneumonia in CXRs was analyzed.

The work contributes to the following objectives-

- The proposed research work aims to implement a federated deep learning-based pneumonia detection model to affirm data privacy protection by utilizing a multi-client federated architecture.

- This work emphasizes the significance of distributed federated learning in healthcare applications and introduces a decentralized federated learning approach using an InceptionV3 model for enhancing privacy and dealing with data heterogeneity. The dataset has been homogenously and heterogenously provided to the participating clients in the network.
- The proposed model effectively addresses data privacy challenges by enabling decentralized model training and also ensures high performance across diverse and non-uniform datasets, making it suitable for sensitive healthcare applications in real-world scenarios.

The remaining article contains Section 2, which discusses the existing models for disease detection. Section 3 provides a description of the methodology and pneumonia dataset. The findings of distributed FL have been presented in Section 4. Finally, the major findings and conclusion of the work are presented in Section 5.

2. Literature Review on Federated Learning Techniques for Disease Detection

In Sharma et al. (2025), the authors employed a FL-based MLP model for pneumonia prediction with IID data in 3 and 4 clients. The results show that the smaller number of clients show improved accuracy; however, the increase in client value decreases the performance and increases the computational time. The model proposed by Sharma & Guleria (2025) has been employed with IID and non-IID distributions in a 5-client federated framework. The authors used FedAVG and FedProx techniques to aggregate the updates collected from each client. The outcomes show that the model improved when the aggregation was changed from FedAVG to FedProx. In Pan et al. (2024), the authors developed a FL model for pediatric pneumonia detection using FedAVG aggregation. The dataset was collected from online repositories containing pneumonia and normal CXRs of 5232 images. The base model for developing this framework was set to VGG11 with the pre-trained weight values of the mageNet dataset. In Alfiansyah et al. (2024), four variants of the CNN model are utilized for pneumonia identification in CXRs. These models were DenseNet, ResNet, Inception, and VGG, out of which the highest performance has been resulted by the DenseNet model. The image pre-processing technique called data balancing fully and partially was also applied, and it has been further implemented with the DenseNet model. In Shiri et al. (2024), the authors worked on covid-19 detection using a decentralized FL framework. The dataset contains 3055 cases which have been further distributed randomly to various clients involved in the FL framework. The DenseNet model has been trained to predict the presence of Covid-19, among which an accuracy of 75% has been identified. In Kandati & Gadekallu (2023), FL-based PSO algorithm has been developed for Covid-19 detection. To develop this model, the authors used a FedAVG aggregation method, where the 10 clients were used for the framework development. The hyperparameters such as learning rate of 0.020, epoch of 30, local model epoch of 5, and utilization of client have been set to 0.1, 0.2, 0.5, and 1.

In Mabrouk et al. (2023), FL-based DL architecture has been introduced, which uses DenseNet121, Inceptionv3, Xception, MobileNetV2, ResNet50, VGG16, ResNet152v2, and DenseNet169 models for training the clients locally. Further, the best performing two models have been aggregated to develop an ensemble model to be applied as a global model. In the work proposed by Kareem et al. (2023), the authors used DenseNet, Alexnet, ResNet50, VGG19, and Inception in the FL-based distributed environment to predict pneumonia. The CXR dataset has been curated and contains 5956 images, which have been further used for the models' training and testing purposes. The comparison of all the base models has shown that ResNet50 outperformed all the others with the highest accuracy. In Malik et al. (2023), DenseNet169, VGG16, and VGG19 have been used with FL architecture for Covid-19 detection in CXRs. The model has been named DMFL_Net, which is applied to the dataset containing 17,301 images collected from different sources having classes, namely, TB, Covid-19, pneuTH, pneu, lung cancer, and normal. The work presented in Riedel et al. (2023) has been implemented using a FL framework with ResNetFed and ResNet50 models

with 5-client architecture. The data was divided among the clients in a heterogeneous manner, where each client had a different sort and distribution of the data. The outcome of the model depicts that the highest performance has been achieved by the ResNetFed model with an overall accuracy of 82.82%. In Subashchandrabose et al. (2023), the authors used neural networks in FL architecture to detect lung cancer in CT scan images. The client value has been set to 5, 10, 20, 40, 80, and 160, and the aggregation technique has been set to FedAVG. In Farkaş et al. (2023), the VGG16 model has been implemented for pneumonia detection, where the FL architecture is applied in 10 client's architecture. The dataset curated from Kaggle contained 5863 images, divided into 10 shards for each client. The images have been resized into 150X150, which is not the accurate and correct input dimension to the VGG16 model, hence may result in optimally for pneumonia detection in the CXRs. In Makkar & Santosh (2023), the authors developed a SecureFed model using an FL-based framework, where the client is kept as 10, 20, 30, 50, and 100. The dataset utilized contains 4200 images, which have been distributed in different ratios to each client.

Table 1 tabulates the techniques, dataset, hyperparameters, summary, and research gaps of the existing studies used for disease detection using FL architecture.

Table 1. A discussion on existing disease detection models implemented using federated learning-based architecture.

References	Techniques	Images	Hyperparameters	Summary	Research gaps	Disease
Sharma et al. (2025)	MLP	Pooled dataset of 10,440 CXRs	Learning rate: 0.0001, Epoch: 10, Batch Size: 32, Clients: 3 and 4, Rounds: 100	The FL-based model has been implemented with a pooled dataset containing higher class imbalance, distributed among 3 and 4 clients in an IID manner.	The model has been employed for IID distribution; however, non-IID data can be explored.	Pneumonia
Sharma & Guleria (2025)	EfficientNetB3	4000 CXRs	Learning rate: 0.001, Epoch: 5, Batch Size: 32, Clients: 5, Rounds: 15	The FL-EfficientNetB3 model has been implemented in IID and non-IID distributions, where the aggregation strategies have been changed to FedAVG and FedProx.	The authors have achieved good results with FedAVG and FedProx aggregations; however, future research may explore other aggregation strategies.	Pneumonia
Pan et al. (2024)	VGG11	5,232 images	Learning rate: NM, Epoch: NM, Batch Size: NM, Clients: 10, Rounds: 100	The model has been proposed for pediatric pneumonia detection in CXRs using FL, where the base model was configured to VGG11.	As per the images used for the implementation, the number of clients has been set to too high value, which may result in the undertraining of the model of the client receiving a lesser number of images.	Pediatric pneumonia
Alfiansyah et al. (2024)	Inception, DenseNet, VGG, ResNet	RSNA-15863 images Mendeley-5856 images	Not Mentioned	The dataset to be used for the implementation was collected from two sources, Mendeley and RSNA. The prediction outcomes have identified that the DenseNet model outperforms by achieving the highest accuracy.	There is a lack of information on the hyperparameter configuration, which makes it difficult for other researchers to develop a similar type of model for disease detection.	Pneumonia

Table 1 continued…

Shiri et al. (2024)	DenseNet	3055 images	Learning rate: 0.00001, Epoch: 300, Batch Size: NM Clients: NM	The DenseNet model is utilized for covid-19 prediction, where the accuracy of 75% and 76% have been identified with the FL and centralized DenseNet model, respectively.	The dataset used by the authors is small, which may provide overfitting concerns in the results.	Covid-19
Kandati & Gadekallu (2023)	PSO	Dataset1: 317 images, Dataset2: 5856 images, Dataset3:	Clients: 10, Aggregation technique: FedAVG and FPS, Epoch: 30, Batch size: 10	The PSO model has been utilized for covid-19 disease detection using a decentralized FL-based framework.	The dataset used for the covid-19 detection is small for the model implementation as the authors have created an architecture containing 10 clients, which depicts that if the client utilization has been set to 1, each client will get a small dataset for training the local model.	Covid-19
Mabrouk et al. (2023)	DenseNet121, Inceptionv3, Xception, Mobilenetv2, resnet50, Vgg16, Resnet152v2 densenet169	5856 images	Learning rate: 0.00001, Epoch: 20, Batch size: 16, Optimizer: Adam	The authors developed a federated ensemble model for pneumonia detection using the combination of the two pre-trained models.	The configuration of the learning rate has been set to a small value of 0.00001, which may result in slow convergence and precision issues and may get stuck in local minima.	Pneumonia
Kareem et al. (2023)	DenseNet, Alexnet, ResNet50, VGG19, Inception	5856 images	Epoch: 20	The authors utilized five pre-trained models for FL-based framework development, among which the ResNet50 has resulted as the best-performing model for pneumonia detection.	The dataset used for the model implementation is 5856 images; however, the data balancing is a major concern, which may result in model bias, overfitting, and increased model complexity.	Pneumonia
Malik et al. (2023)	DenseNet169, VGG16, VGG19	17,301 images	Epoch: 100, Clients: 3	Three models, namely, DenseNet169, VGG19, and VGG16 have been applied in FL for multiclass classification of TB, PneuPH, Pneu, covid-19, and lung cancer.	The work lacks detailed information on hyperparameter configuration.	Tuberculosis, Covid-19, Pneumonia, lung cancer.
Riedel et al. (2023)	ResNet50, ResNetFed	1411 images	Clients: 5, Aggregation technique: FedAVG, Epoch: 100, Batch size: 6, Optimizer: SGD+momentum, Momentum: 0.1, Learning rate: 0.0005	The model was built for pneumonia detection in centralized and decentralized frameworks.	A small dataset has been provided to five clients in a heterogeneous configuration; however, the dataset contains fewer images. The dataset is also imbalanced, which may result in misleading metrics.	Pneumonia

Table 1 continued…

Subashchand rabose et al. (2023)	Neural networks	206 images	Aggregation technique: FedAVG, Clients: 5, 10, 20, 40, 80, and 160	The model is implemented for cancer detection in lung CT scan images using FL approach.	In this work, the details about the data distribution among the clients have not been provided. Further, the lack of information regarding hyperparameter configuration also limits the work.	Lung cancer
Farkaş et al. (2023)	VGG16	5863 images	Clients: 10, Optimizer: SGD	The VGG16 base model is utilized in 10 clients' FL frameworks for pneumonia detection.	The authors have used only IID distribution of the data among clients; however, this is a challenge in real-life scenarios as different hospitals have different sorts of datasets with different ratios.	Pneumonia
Makkar & Santosh (2023)	FedSecure	4200 images	Clients: 10, 20, 30, 50, and 100, Aggregation technique: FedAVG, FedMGDA+, and FedRAD, Optimizer: SGD	The pneumonia detection model has been developed by using a FL framework, where the data distribution is kept as heterogeneous.	The authors have divided the dataset into five different scenarios, where each scenario is client-based. The authors used a segment of the dataset containing 200, 400, 600, 1000, and 2000 for 10, 20, 30, 50, and 100 client architecture, respectively. This distribution may result in-optimally due to less number of images in each client-based scenario.	Covid-19, pneumonia, and normal

3. Material and Methods

A detailed explanation of the utilized dataset and the proposed InceptionV3 in a centralized DL and decentralized FL has been presented in this section.

A. Dataset

The proposed model utilizes two pneumonia detection datasets curated from Kaggle (Mooney, 2018; Patel, 2020). The dataset in Patel (2020) possesses 6431 images of normal, pneumonia, and Covid-19 classes, whereas the dataset presented in Mooney (2018) has 5856 images of pneumonia and normal lungs. The class distribution in each dataset was not balanced; hence, two datasets were pooled, and balancing was performed. The outcome of pre-processing contains 4296 images with an equal number of pneumonia and normal CXRs in train and test folders.

B. Proposed methodology for pneumonia detection

This work implements the InceptionV3 model in a centralized DL and distributed FL with IID and non-uniform distributions. The InceptionV3 is a contemporary neural network architecture that has a high level of accuracy in image recognition and classification tasks. In the initial phase of the model development, an Inception model was developed, which is contained within a GoogleNet model (Sharma et al., 2023). It is

the series of the model that won the ImageNet Large Scale Visual Recognition Challenge (ILSVRC) in 2014. Inception models are efficient due to the availability of the resources to make the calculations and computations in real-time and also involve fewer parameters in the learning process. The convolutional layers in the model are flexibly designed so that a threshold operation can act as an activation function to reduce operations (Wang et al., 2019). This increases the performance of the model as well as efficacy by taking less computations. The InceptionV3 diminishes the size of the receptive field by making different sizes of filters, such as (3x3 followed by 1x3 or 3x1) instead of large sizes of 5x5, unlike a typical convolutional neuron layer. The InceptionV3 model is also efficient and faster in terms of converging time; there is an alteration in the training procedure with the addition of auxiliary classifiers (Joshi et al., 2020). These classifiers exert an effect on hidden levels of the model because each node of the layer weighs additional amounts of gradients. The stride convolutions are used together with the stride pooling component to obtain detailed features. The grouping samples are used to reduce the information loss during the computation. Since the model contains an increased number of neurons, the hidden layers are more complex. Batch normalization is one of the most popular forms of regularization, followed by InceptionV3, which can train the model fast and achieve better results by decreasing the covariate shift. InceptionV3 is the successor to the Inception model that refines the inception modules. The block has two units of Inception's network, with each containing several types of convolution layers. This structure makes the model generalize the information of a wide range of scales, which makes the model approximate the true level. Improved factorization using convolutions and asymmetric convolutions in the module design captures complex features and patterns in the images, resulting in optimal performance and ideal model development. In the proposed work, centralized DL and distributed FL have been implemented for pneumonia detection.

- ***Centralized deep learning-based InceptionV3***

Figure 1 illustrates the proposed centralized deep learning-based InceptionV3 for pneumonia detection. The InceptionV3 model has been implemented in a centralized framework, where the dataset has been collected at the central server to implement the model. This model has been configured with the key hyperparameters, namely, batch size, optimizer, epochs, and learning rate as 64, Adam, 10, and 0.001, respectively. The collected images were of different sizes, which were resized to a uniform and standard input image size of 299x299. The centralized DL requires extensive data collected at a centralized location, which creates a concern due to privacy issues in collecting medical data of the patients. The proposed methodology for centralized InceptionV3 model implementation has been provided in **Figure 1**.

- ***Distributed federated learning-based InceptionV3***

Figure 2 illustrates the proposed distributed federated learning-based InceptionV3 model for IID and non-IID data distribution in 5 clients. The problem associated with the traditional DL model is that it works with the centralized framework, which needs a large volume of data to predict pneumonia optimally. However, the collection of the healthcare dataset is a challenging task, as it contains the patient's sensitive information, which is not allowed to be shared outside the hospital due to strict regulations provided by the HIPAA Act in 1996. On the other hand, the advancements in the traditional DL models have led to the development of distributed FL, which does not store the dataset in a centralized location; instead, it creates the model at the server and sends it to each hospital for computation, which then results in the updated model parameter in return to the centralized location. In this way, the FL framework doesn't exploit the patient's privacy, which also results in optimal model development. In the IID distribution, individual clients have been assigned the same distribution of the data, and the data itself remains different. In the non-IID distribution, the complete data has been independently distributed to the clients with varying ratios and different sets of CXRs. This framework has utilized the complete number of clients participating in the process. The configured key hyperparameters are tabulated in **Table 2**.

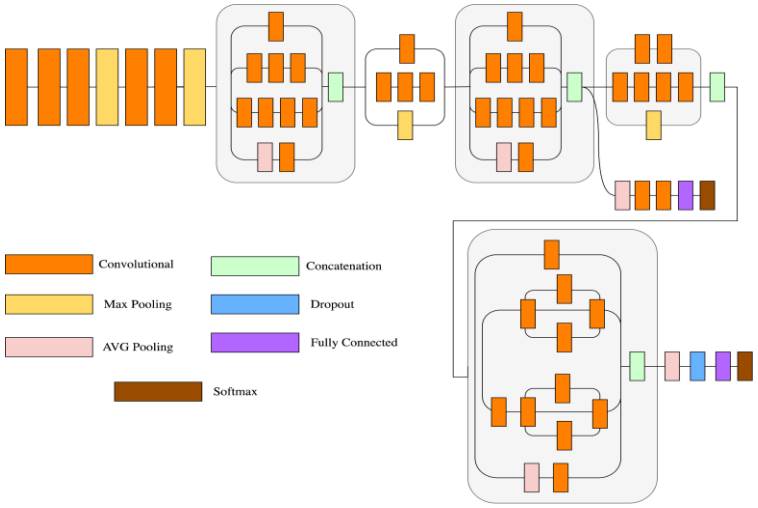

Figure 1. Centralized InceptionV3 model for pneumonia detection.

Table 2. Key hyperparameters configurations for the FL-based InceptionV3 model development.

Hyperparameters	**Value**	**Hyperparameters**	**Value**
Clients	5	Client Utilization	100%
Batch Size	32	Train: Test Ratio	80:20
Local: Global Epochs	1:1	Optimizer	Adam
Learning Rate	0.001	Loss Metric	Sparse categorical cross-entropy
Rounds	25	Classes	2
Input Image Size	299X299	Data Distribution	IID and Non-IID
Seed	123	Aggregation Technique	FedAVG
Dense Activation	ReLU	Prediction Activation	SoftMax

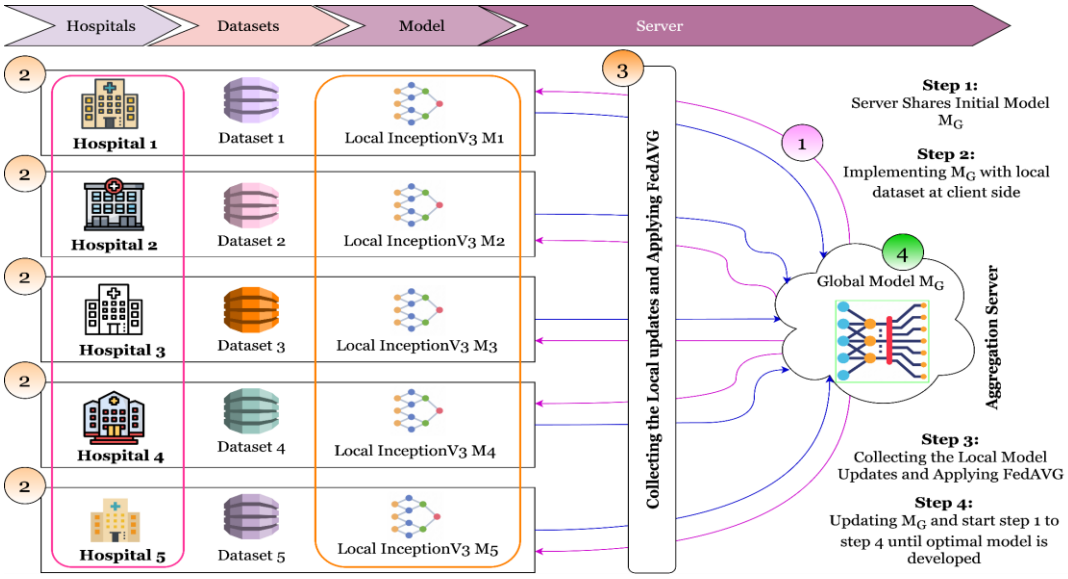

Figure 2. Distributed federated learning-based InceptionV3 model for pneumonia detection.

4. Results and Discussion

This section discusses the proposed centralized and distribution federated learning results when implemented with the InceptionV3 model.

A. Results of the centralized deep learning-based InceptionV3 model

This section provides the findings of the InceptionV3 model when implemented with centralized deep learning. The results show the performance outcomes in terms of accuracy, loss, precision, recall, and F1-score.

Figure 3 represents the accuracy of the centralized deep learning InceptionV3 model. This graph depicts the highest training accuracy of 90.68% at epoch 9, whereas the highest accuracy in testing has been achieved at 90.49% at epoch 10.

Figure 3. Accuracy of the centralized deep learning InceptionV3 model.

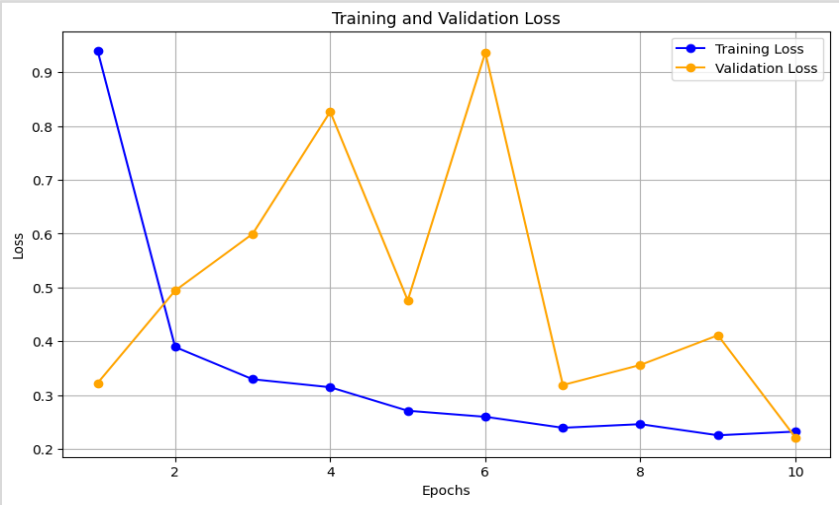

Figure 4. Loss of the centralized deep learning InceptionV3 model.

Figure 4 shows the loss of the centralized DL InceptionV3 model at the training and testing phases. The highest training loss and testing loss of 0.9405 at epoch 1 and 0.9363 at epoch 6, respectively, whereas the lowest training loss of 0.2253 and testing loss of 0.221 have been analyzed at epochs 9 and 10, respectively. **Figure 5** depicts the precision of the centralized DL InceptionV3 model. The highest precision at training and testing are 0.9086 and 1 at epochs 8 and 1, whereas the lowest precision values have been found as 0.7497 and 0.9135 at epoch 1 for both the train and test phases.

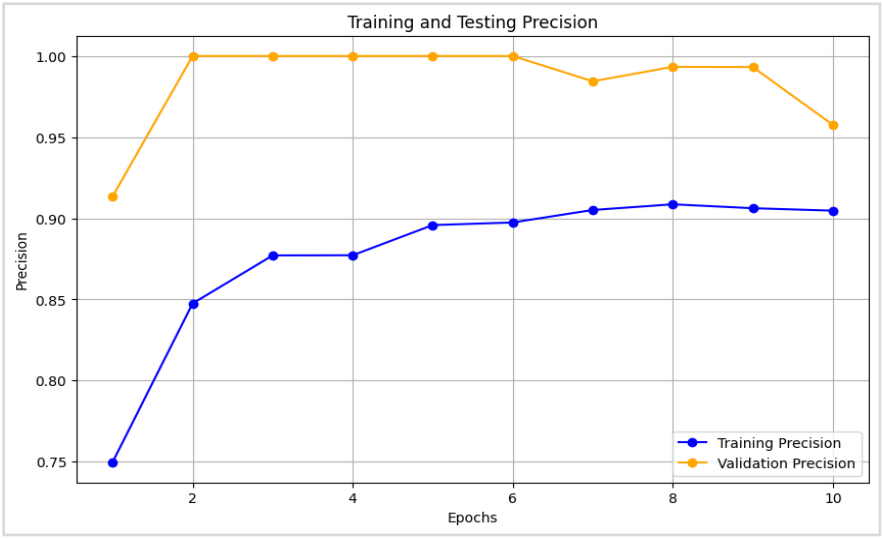

Figure 5. Precision of the centralized deep learning InceptionV3 model.

Figure 6 represents the recall of the centralized DL InceptionV3 model. The highest recall of 0.9057 and 0.8474 have been found at epochs 9 and 10, whereas the lowest recall of 0.7141 and 0.2488 have been found at epochs 1 and 6 in the training and testing phases, respectively.

Figure 6. Recall of the centralized deep learning InceptionV3 model.

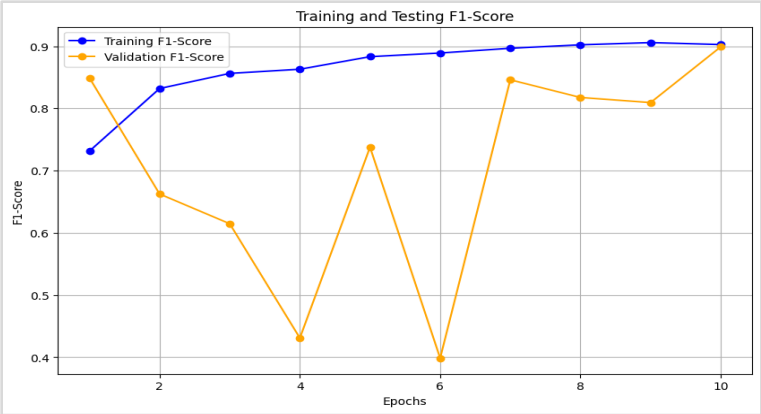

Figure 7. F1-score of the centralized deep learning InceptionV3 model.

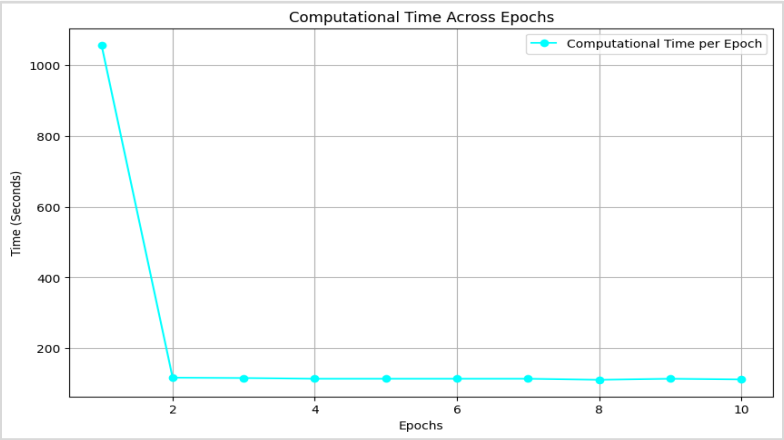

Figure 8. Computational time of the centralized deep learning InceptionV3 model at each epoch.

Figure 7 represents the F1-score of the centralized DL InceptionV3 model. The highest value of the F1-score is identified as 0.9059 and 0.8991 at epochs 9 and 10, whereas the lowest recall of 0.7315 and 0.3985 have been found at epochs 1 and 6 in the training and testing phases, respectively. **Figure 8** depicts the communication time of the centralized deep learning InceptionV3 model at each epoch. The highest communication time was taken by epoch 1, which was reduced in epochs 2-10.

B. Results of the distributed federated learning-based InceptionV3 model

This section provides the results of the InceptionV3 model when implemented with distributed FL with respect to IID and non-IID data distribution.

- ***Results of the distributed federated learning with the InceptionV3 model with respect to IID data distribution***

This section represents the findings of the proposed distributed FL model while applied with the uniform distribution of the data. The clients participating in this framework contain a similar ratio of data; however, the data within the client itself is different from the data at another client.

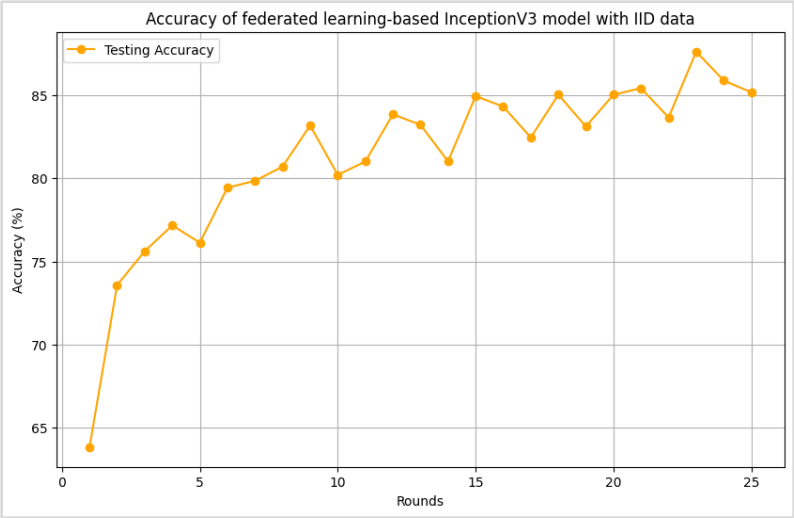

Figure 9. Accuracy of distributed federated learning-based InceptionV3 model with IID data distribution.

Figure 9 depicts the accuracy of the distributed FL model with IID data distribution, where the highest accuracy has been identified as 87.62% at round 23, whereas the least accuracy value was resulted as 63.81% at round 1.

Figure 10 represents the loss of the distributed FL InceptionV3 model with IID data distribution. The highest loss and lowest loss of 8.7924 and 0.4041 were identified at rounds 1 and 23, respectively. **Figure 11** depicts the recall of the distributed FL model with IID data distribution. The highest recall and lowest recall of 0.8635 and 0.6141 were achieved in rounds 23 and 1, respectively.

Figure 12 illustrates the precision value of the proposed distributed FL model with uniform data distribution in 5 clients' architecture. The highest precision of 0.8821 and lowest of 0.6364 have been identified at rounds 23 and 1, respectively.

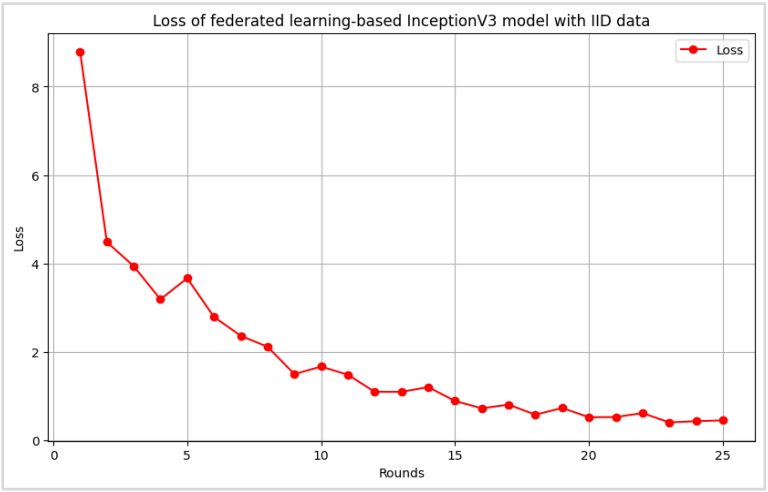

Figure 10. Loss of distributed federated learning-based InceptionV3 model with IID data distribution.

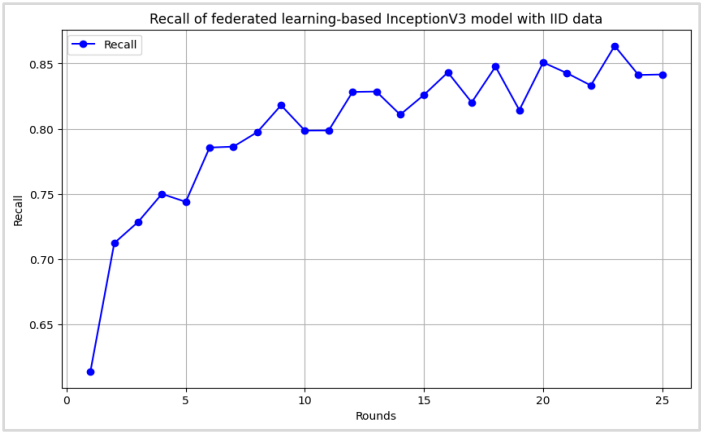

Figure 11. Recall of distributed federated learning-based InceptionV3 model with IID data distribution.

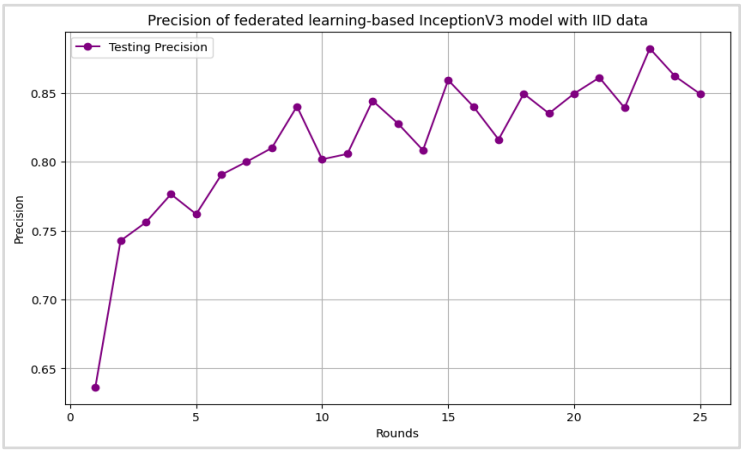

Figure 12. Precision of distributed federated learning-based InceptionV3 model with IID data distribution.

Figure 13 shows the F1-score value of the proposed distributed FL model with uniform data distribution in 5 clients' architecture. The highest precision of 0.8727 and lowest of 0.6251 have been achieved at rounds 23 and 1, respectively.

Table 3 tabulates the performance outcomes of the distributed FL model with IID data distribution. The summary of the outcomes has been tabulated in terms of client-wise recall, accuracy, lowest computational time, precision, highest computational times, etc.

Figure 14 shows the client-wise accuracy of the proposed distributed FL-based InceptionV3 model with the IID data distribution. This illustrates that client 2 achieves the highest accuracy of 90.44% at round 23, whereas clients 1, 3, 4, and 5 shows 88.24%, 87.13%, 86.95%, and 88.10%, respectively.

Figure 15 shows the client-wise loss of the proposed distributed FL model with the IID data distribution with respect to increasing rounds. The highest loss of 10.0784 has been identified by client 2, whereas the lowest loss of 0.2812 has also resulted by client 2.

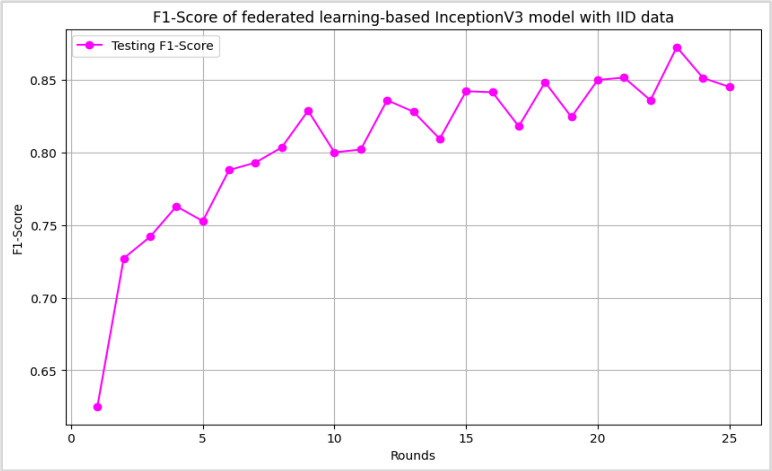

Figure 13. F1-score of distributed federated learning-based InceptionV3 model with IID data distribution.

Table 3. Performance outcomes of the distributed federated learning-based InceptionV3 model with IID data distribution.

Client/Performance	Client 1	Client 2	Client 3	Client 4	Client 5
Round	21	23	24	20	13
Highest accuracy	88.24%	90.44%	87.13%	86.95%	88.10%
Round	1	1	1	1	1
Highest loss	9.6251	10.0784	8.8882	8.0746	7.2959
Round	23	23	24	21	23
Lowest loss	0.3383	0.2812	0.4089	0.4397	0.3833
Round	19	22	22	22	22
Highest precision	0.8813	0.8984	0.8740	0.8622	0.8947
Round	19	22	16	20	9
Highest recall	0.8750	0.8984	0.8473	0.8726	0.8806
Round	22	22	18	20	8
Highest F1-score	0.8727	0.8984	0.8450	0.8726	0.8806
Round	1	1	1	1	1
Highest computational time	113 seconds	59 seconds	61 seconds	66 seconds	47 seconds
Round	4, 5, 14, 15, 16, 19, 21, 22	12, 13, 19, 20, 21, 23, 24	15, 17, 18, 19, 20, 21, 23, 24	4, 5, 14, 15, 16, 19, 21, 22, 23, 24, 25	1, 8, 11, 12, 14, 16, 19, 20, 21, 22, 23, 24, 25
Lowest Computational Time	10 Seconds	13 Seconds	16 Seconds	19 Seconds	22 Seconds

Figure 16 depicts the client-wise recall values of the proposed distributed FL model with the IID data distribution. The highest recall value of 0.8984 has been identified by client 2 at round 22. **Figure 17** shows the client-wise precision values of the proposed distributed FL model with the IID data distribution. The highest precision value of 0.8984 has been identified by client 2 at round 22.

Figure 18 depicts the client-wise F1-score values of the proposed distributed FL model with the IID data distribution. The highest F1-score value of 0.8984 has been identified by client 2 at round 22.

Figure 19 shows the client-wise computational time of the proposed distributed FL model with the IID data distribution. The highest and lowest computational time of 113 seconds has been taken by client 1, whereas the lowest computational time has also been taken by client 1 at rounds 4, 5, 14, 15, 16, 19, 21, and 22.

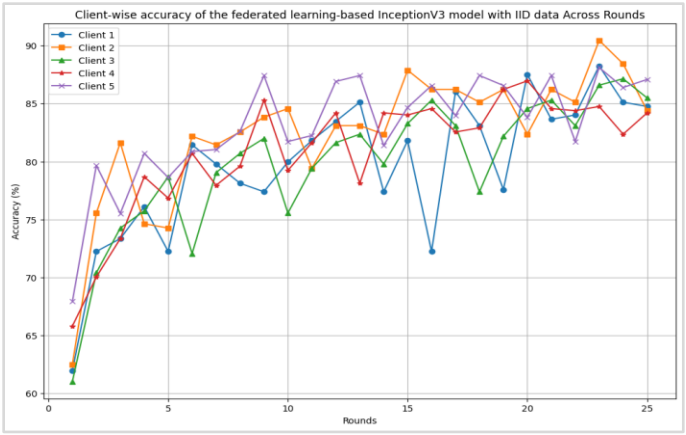

Figure 14. Client-wise accuracy of the distributed FL InceptionV3 model with the IID data distribution.

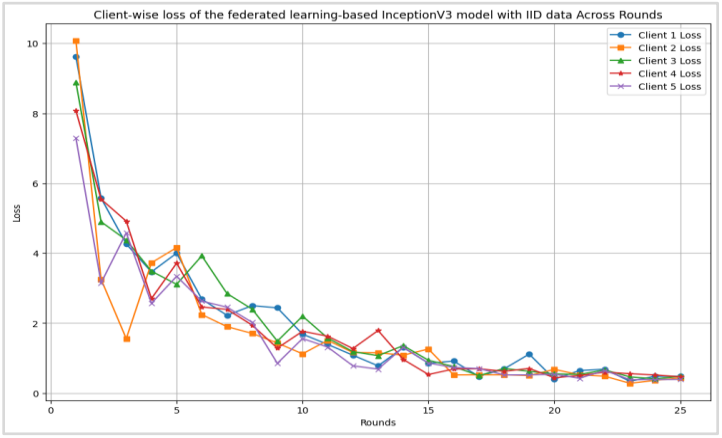

Figure 15. Client-wise loss of the distributed FL InceptionV3 model with the IID data distribution.

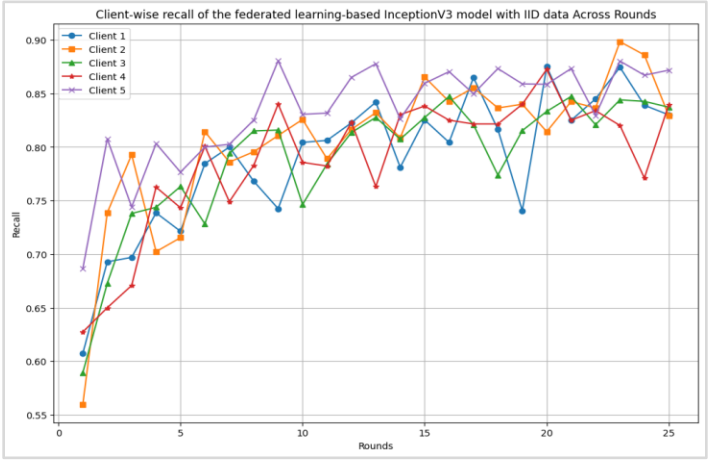

Figure 16. Client-wise recall of the distributed FL InceptionV3 model with the IID data distribution.

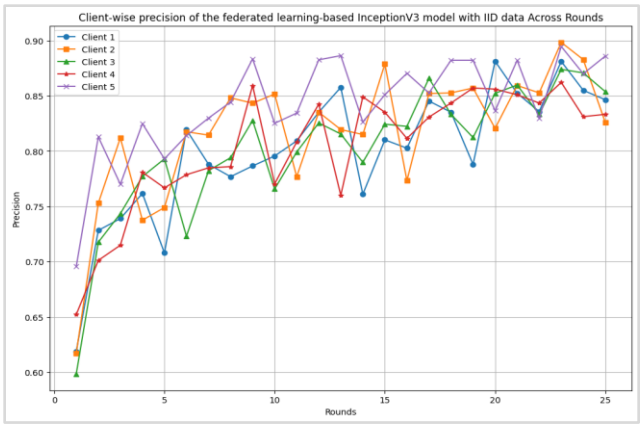

Figure 17. Client-wise precision of the distributed FL InceptionV3 model with the IID data distribution.

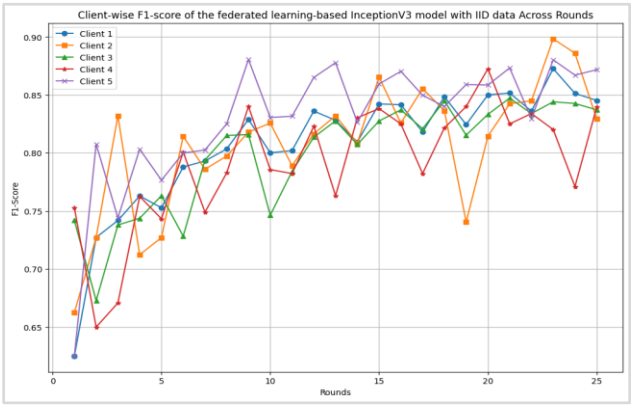

Figure 18. Client-wise F1-Score of the distributed FL InceptionV3 model with the IID data distribution.

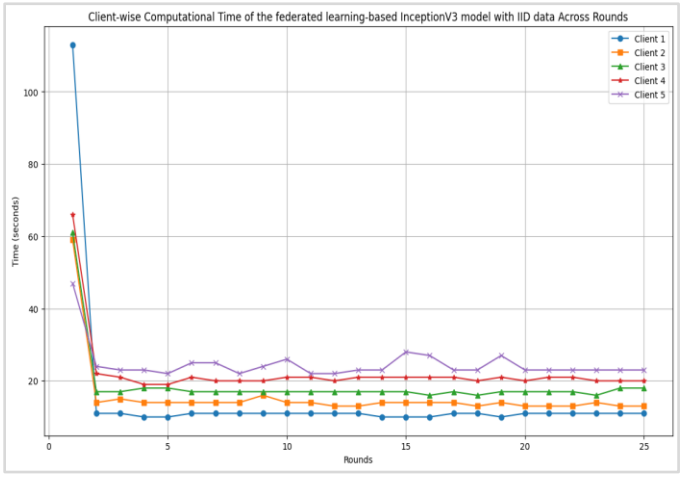

Figure 19. Client-wise computational time taken by the distributed FL InceptionV3 model with the IID data distribution.

- ***Results of the distributed federated learning-based InceptionV3 model with respect to non-IID data distribution***

This section discusses the findings of the proposed distributed FL model while applied with a non-uniform distribution of the data. The data for each client has been provided in different distributions, and the data itself is different at each client.

Figure 20 shows the accuracy of the distributed federated learning with the InceptionV3 model with respect to non-IID data distribution. The highest accuracy of 86.15% and lowest accuracy of 65.84% were identified in rounds 23 and 1, respectively. **Figure 21** depicts the loss value of the proposed FL InceptionV3 technique implemented in non-IID data distribution. The highest loss of 8.0069 and lowest loss of 0.4139 were identified in rounds 1 and 23, respectively.

Figure 22 illustrates the recall value of the proposed InceptionV3 model implemented in non-IID data distribution using FL. The highest and lowest recalls of 0.8483 and 0.6335 have been identified at rounds 23 and 1, respectively. **Figure 23** illustrates the precision values achieved using the FL-based InceptionV3 model implemented in non-IID data distribution. The highest precision of 0.8670 and lowest precision of 0.6593 were identified in rounds 23 and 1, respectively.

Figure 24 depicts the F1-score of the proposed InceptionV3 model implemented in non-IID data distribution using FL. Rounds 23 and 1 show the highest and lowest F1-score values of 0.8576 and 0.6461, respectively.

Table 4 depicts the performance outcomes of the distributed FL model with non-IID data distribution. The summary of the outcomes has been tabulated in terms of client-wise recall, accuracy, lowest computational time, precision, highest computational times, etc.

Figure 25 shows the client-wise accuracy of the proposed FL-based InceptionV3 model implemented with non-IID data distribution. The highest accuracy was achieved by client 3 as 88.79%, whereas client 1, client 2, client 4, and client 5 identified 86.03%, 87.87%, 86.03%, and 88.28%, respectively.

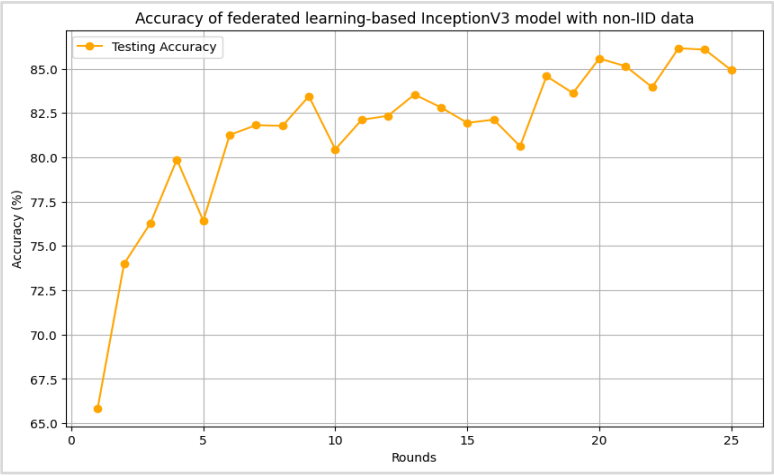

Figure 20. Accuracy of distributed FL InceptionV3 model with non-IID data distribution.

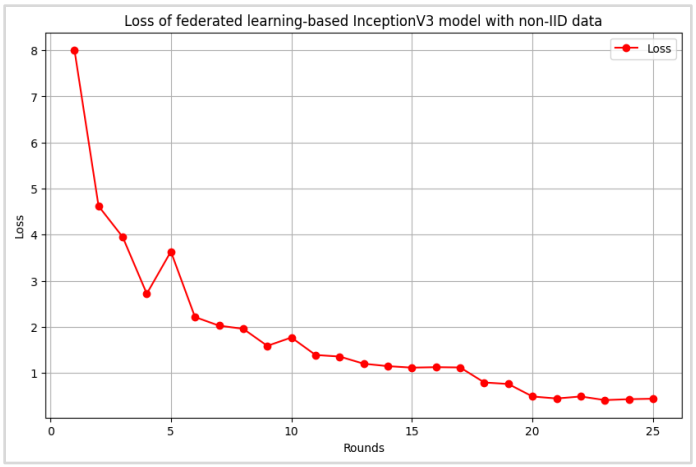

Figure 21. Loss of distributed FL InceptionV3 model with non-IID data distribution.

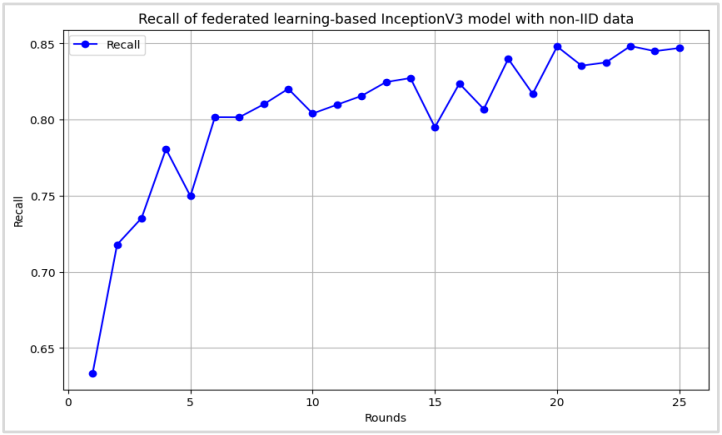

Figure 22. Recall of distributed FL InceptionV3 model with non-IID data distribution.

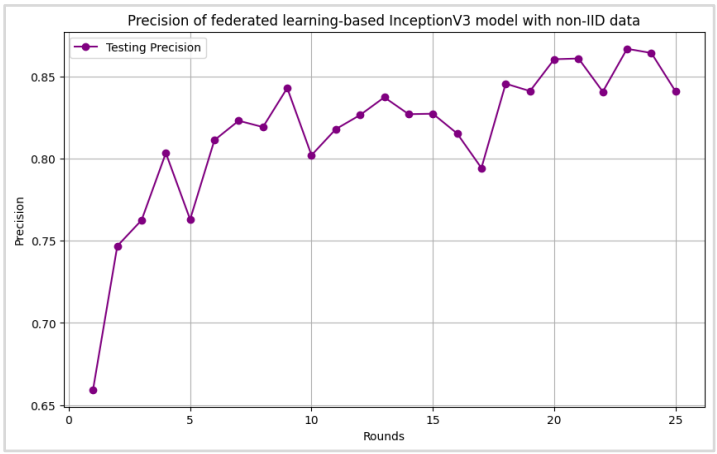

Figure 23. Precision of distributed FL InceptionV3 model with non-IID data distribution.

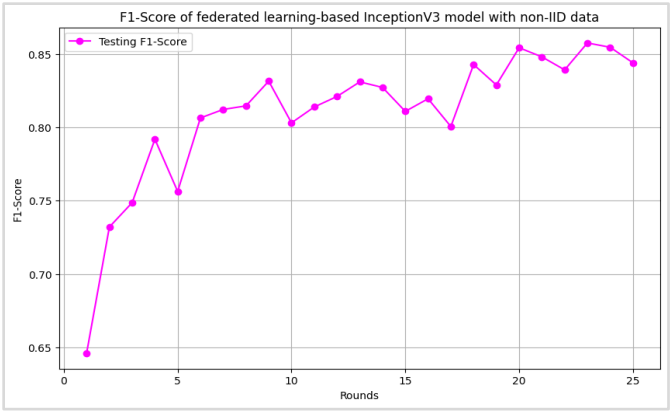

Figure 24. F1-score of distributed FL InceptionV3 model with non-IID data distribution.

Table 4. Performance outcomes of the distributed FL InceptionV3 model with non-uniform data distribution.

Client/Performance	Client 1	Client 2	Client 3	Client 4	Client 5
Round	22	21	24	6	23
Highest accuracy	86.03%	87.87%	88.79%	86.03%	88.28%
Round	1	1	1	1	1
Highest loss	10.5232	5.9728	9.0291	9.2973	5.2121
Round	25	23	24	20	20
Lowest loss	0.3623	0.2793	0.353	0.3663	0.3514
Round	23	22	23	14	22
Highest precision	0.8605	0.904	0.8880	0.8725	0.8977
Round	24	22	23	19	22
Highest recall	0.8533	0.8828	0.8629	0.8726	0.8803
Round	23	23	23	19	9
Highest F1-score	0.8674	0.8882	0.8655	0.8544	0.8847
Round	1	1	1	1	1
Highest computational time	122 seconds	70 seconds	72 seconds	75 seconds	52 seconds
Round	3	8	7	3	5
Lowest Computational Time	9 Seconds	12 Seconds	15 Seconds	18 Seconds	20 Seconds

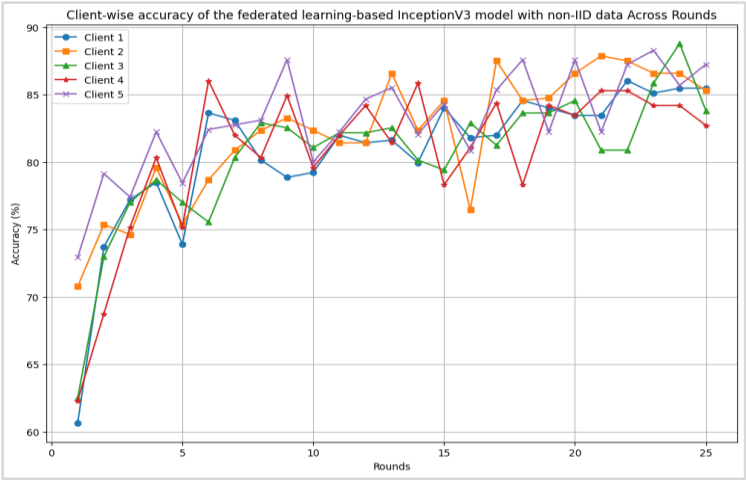

Figure 25. Client-wise accuracy of the distributed FL InceptionV3 model with the non-IID data distribution.

Figure 26 illustrates the client-wise loss of the proposed FL-based InceptionV3 model implemented with non-IID data distribution. The highest loss was identified by client 1 as 10.5232, whereas the lowest loss value was identified by client 2 as 0.2793 at round 23. **Figure 27** depicts the client-wise recall of the model with the non-IID data distribution. The highest and lowest recall values of 0.8828 and 0.8533 were obtained by clients 2 and 1, respectively.

Figure 28 shows the client-wise precision of the proposed FL-based InceptionV3 model with the non-IID data distribution. The highest and lowest precisions were for clients 2 and 1, which were 0.904 and 0.8605, respectively. **Figure 29** illustrates the client-wise F1-score of the proposed model with the non-uniform data distribution. The highest and lowest F1 scores were for clients 2 and 4, which were 0.8882 and 0.8544, respectively.

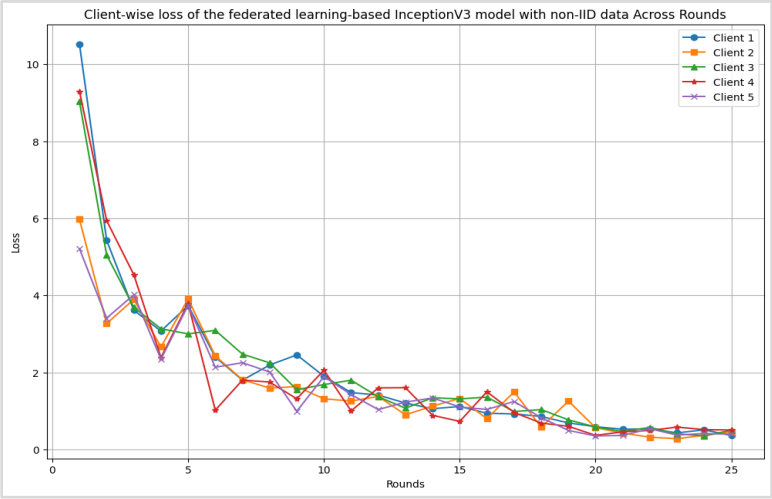

Figure 26. Client-wise loss of the distributed FL InceptionV3 model with the non-IID data distribution.

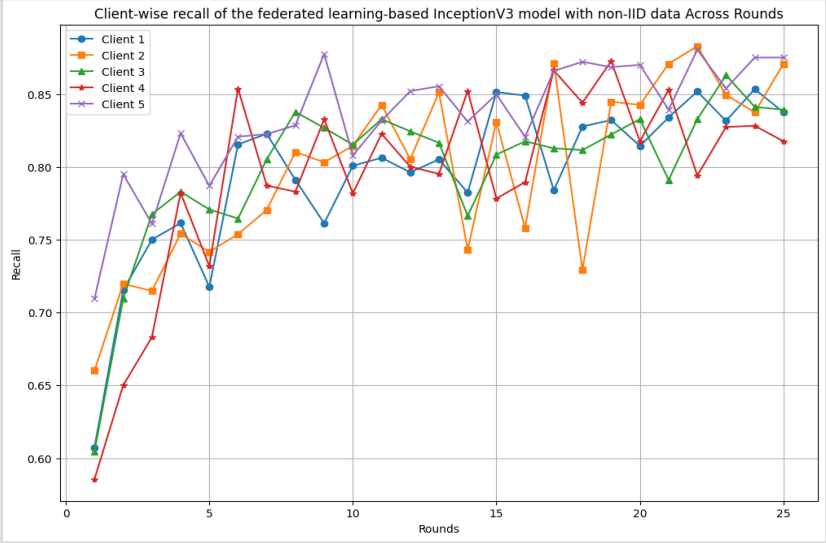

Figure 27. Client-wise recall of the distributed FL InceptionV3 model with the non-IID data distribution.

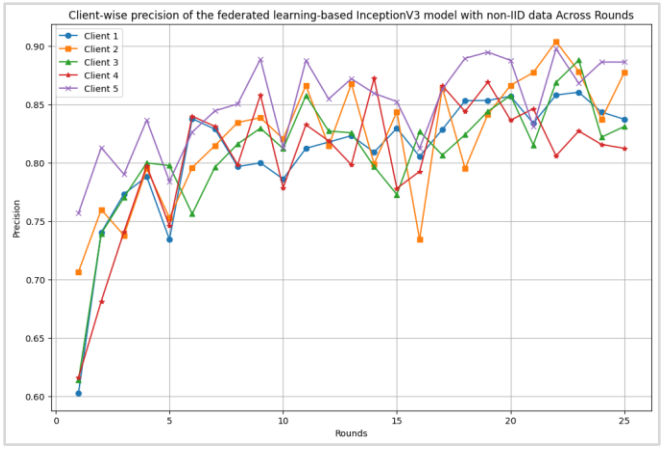

Figure 28. Client-wise precision of the distributed FL InceptionV3 model with the non-IID data distribution.

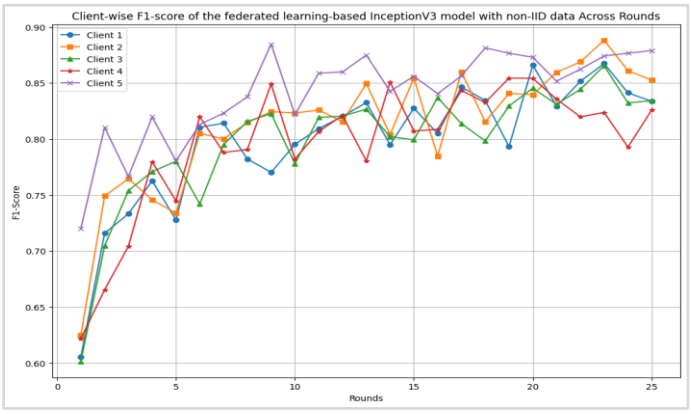

Figure 29. Client-wise F1-Score of the distributed FL InceptionV3 model with the non-IID data distribution.

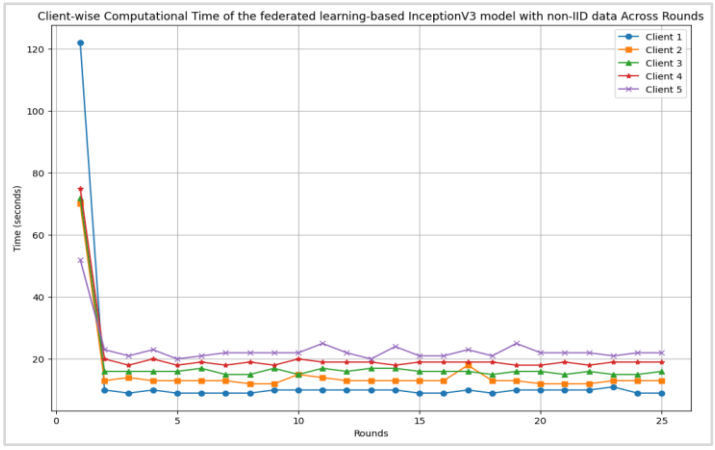

Figure 30. Client-wise computational time taken by the distributed FL InceptionV3 model with the non-IID data distribution.

Figure 30 illustrates the client-wise computational time to perform the implementation at each round by the proposed model with the non-IID data distribution. The highest computational time was taken by round 1 at each client, whereas the lowest computational time was taken by client 1 at round 3 at 9 seconds.

C. Discussion on the performance outcomes achieved by centralized deep learning and distributed federated learning-based InceptionV3 model

This section delves into the discussion of the results identified by the centralized DL-based InceptionV3 and distributed FL-based InceptionV3 model.

Table 5 tabulates the results comparison of centralized DL-based InceptionV3 and distributed FL model.

Table 5. Results comparison of centralized DL-based InceptionV3 and distributed FL-based InceptionV3 model.

Performance/ Framework	**Centralized**	**FL-InceptionV3**	
Parameters	**DL-InceptionV3**	**IID**	**Non-IID**
Accuracy	90.49%	87.62%	86.15%
Lowest Loss	0.221	0.4041	0.4139
Precision	0.9086	0.8821	0.8670
Recall	0.8474	0.8635	0.8483
F1-score	0.8991	0.8727	0.8576

The highest accuracy among centralized DL and FL has resulted in the DL-based InceptionV3 model; however, the DL models have data centralization risks such as less bandwidth efficiency, inability to work with data diversity and privacy concerns. The DL models are incapable of providing optimal performance if the data is not centralized, whereas the FL models work in a distributed manner and send the models to individual hospitals rather than collecting the data at a central location. The strict rules documented by HIPAA are followed in hospitals and health insurance companies that don't allow to share the patient's data. This Act. protects patient privacy, and improves the portability and continuity of health insurance coverage. Hence, centralized DL is not suitable to be used in the medical field. On the other side, the FL framework is developed using DL models, where the distributed architecture is used for disease prediction. The use of FL for medical image analysis is secured and protected. Though the proposed FL-based InceptionV3 provides less accuracy than the centralized model, nevertheless, the variation among these accuracies is small and doesn't depict the worst impact as the model provides extra assistance to the clinicians, and the final decision of the pneumonia detection is confirmed by the doctors.

In addition, the FL-based InceptionV3 is implemented in both IID and non-uniform data distribution scenarios. The performance of the FL-based InceptionV3 model in IID distribution is better than that of non-IID data distribution. However, in real-world scenarios, the hospitals contain different sorts of data, which is applicable to FL-based models implemented with non-IID data distribution. Hence, the proposed model was deployed with the non-uniform data distribution.

In the proposed work, the performance of the IID distribution-based model is better than the non-IID data distribution because the similar distribution of the data made the model more efficient statistically and provided better convergence and stability, whereas, in non-IID data distribution, the data is statistically heterogeneous, and also has the challenges of learning complexity, data segregation issues, and increased risk of model drift.

D. Performance comparisons of the proposed distributed FL-based InceptionV3 model with the existing federated learning-based models

This section contrasts the results of the proposed distributed FL-based InceptionV3 model with the existing FL-based models.

Figure 31 illustrates the performance contrast of the proposed model with the existing FL models. The work presented in Shiri et al. (2024) has used a DenseNet model where the outcomes have been achieved with 75% accuracy. The model presented in Riedel et al. (2023), also obtained an accuracy of 82.82%, which is less in comparison to the proposed distributed FL model implemented with IID and non-uniform data distributions.

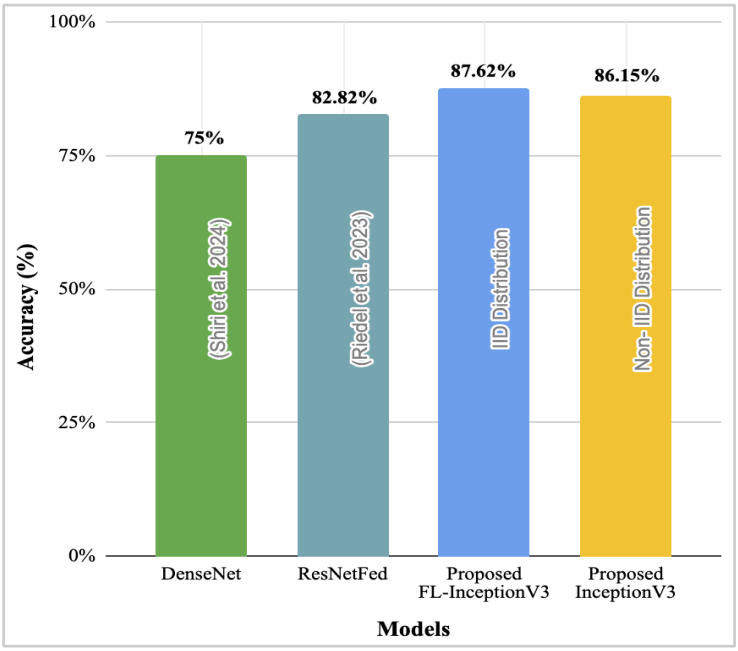

Figure 31. Performance comparisons of the proposed distributed FL InceptionV3 model with the existing FL-based models.

5. Conclusion

The increase in Covid-19 cases has resulted in limited medical resources. The advanced stages of this pandemic decrease the secretion, causing the alveoli to collapse, turning into pneumonia. The report provided by WHO revealed that pneumonia affects the most to people over the age of 65 and patients with a weakened immune system. The traditional methods used for pneumonia detection require high expertise and proficiency. The misdiagnosis of the disease results in delayed treatment, worsening the health condition and increasing the mortality rates. In the proposed work, centralized deep learning and distributed federated learning have been implemented using a pre-trained and fine-tuned InceptionV3 model. The centralized deep learning model has been configured with the key hyperparameters, namely, batch size, optimizer, epochs, and learning rate as 64, Adam, 10, and 0.001, respectively, whereas the distributed FL-based InceptionV3 has been configured with 5, 32, 0.001, 25, 123, Adam, 100%, and FedAVG for clients, batch size, learning rate, rounds, seed, optimizer, client utilization, and aggregation technique, respectively. The distributed FL-based InceptionV3 model results in an accuracy of 87.62% and 86.15% and a loss of

0.4041 and 0.4139 for IID and non-IID data, respectively. The results of the centralized DL-based InceptionV3 show that the highest accuracy of 90.49% has been achieved; however, this model is highly sensitive to patients' data as it collects the information at the centralized location. Therefore, the FL-based InceptionV3 model can be used to reduce data centralization risks, provide high bandwidth, and work with diverse datasets. In the future, the FL-based InceptionV3 model can be enhanced by increasing the number of local and global epochs and augmenting the existing datasets to achieve optimal result.

Conflicts of Interest

No conflicts of interest have been associated with this publication.

Acknowledgments

The authors would like to thank the editors and reviewers for their valuable comments and suggestions. This research did not receive any specific grant from funding agencies in the public, commercial, or not-for-profit sectors.

AI Disclosure

The author(s) declare that no assistance is taken from generative AI to write this article.

References

Adjei-Mensah, I., Zhang, X., Agyemang, I.O., Yussif, S.B., Baffour, A.A., Cobbinah, B.M., Sey, C., Fiasam, L.D., Chikwendu, I.A., & Arhin, J.R. (2024). Cov-fed: federated learning-based framework for COVID-19 diagnosis using chest X-ray scans. *Engineering Applications of Artificial Intelligence*, *128*, 107448. https://doi.org/10.1016/j.engappai.2023.107448.

Alfiansyah, A., Widiarti, H., Reynaldo, V., Widjaja, W., & Bobelin, L. (2024). A framework for multi institutional collaboration for pneumonia screening by means of federated learning. *Electronics, Communications and Networks*, *381*, 135-142.

Alipoor, S.D., Jamaati, H., Tabarsi, P., & Mortaz, E. (2020). Immunopathogenesis of pneumonia in COVID-19. *Tanaffos*, *19*(2), 79-82.

Alyasseri, Z.A.A., Al-Betar, M.A., Doush, I.A., Awadallah, M.A., Abasi, A.K., Makhadmeh, S.N., & Zitar, R.A. (2022). Review on COVID-19 diagnosis models based on machine learning and deep learning approaches. *Expert Systems*, *39*(3), e12759. https://doi.org/10.1111/exsy.12759.

Darzi, E., Sijtsema, N.M., & van Ooijen, P.M.A. (2024). A comparative study of federated learning methods for COVID-19 detection. *Scientific Reports*, *14*(1), 3944. https://doi.org/10.1038/s41598-024-54323-2.

Farkaş, C.R., Ciobanu, R.I., & Dobre, C. (2023). Pneumonia detection using federated learning. In *2023 24th International Conference on Control Systems and Computer Science* (pp. 160-165). IEEE. Bucharest, Romania. https://doi.org/10.1109/cscs59211.2023.00033.

Goyal, S., & Singh, R. (2023). Detection and classification of lung diseases for pneumonia and Covid-19 using machine and deep learning techniques. *Journal of Ambient Intelligence and Humanized Computing*, *14*(4), 3239-3259.

Gulati, S., Guleria, K., & Goyal, N. (2022). Classification and detection of coronary heart disease using machine learning. In *2022 2nd International Conference on Advance Computing and Innovative Technologies in Engineering* (pp. 1728-1732). IEEE. Greater Noida, India.

Hariri, M., & Avşar, E. (2023). COVID-19 and pneumonia diagnosis from chest X-ray images using convolutional neural networks. *Network Modeling Analysis in Health Informatics and Bioinformatics*, *12*(1), 17. https://doi.org/10.1007/s13721-023-00413-6.

Hasan, M.K., Ahmed, S., Abdullah, Z.E., Khan, M.M., Anand, D., Singh, A., AlZain, M., & Masud, M. (2021). Deep learning approaches for detecting pneumonia in COVID-19 patients by analyzing chest X-ray images. *Mathematical Problems in Engineering*, *2021*(1), 9929274. https://doi.org/10.1155/2021/9929274.

Hatmi, Z.N. (2021). A systematic review of systematic reviews on the COVID-19 pandemic. *SN Comprehensive Clinical Medicine*, *3*(2), 419-436.

Holt, N.R., Neumann, J.T., McNeil, J.J., Cheng, A.C., Unit, H.E., & Prahan, V. (2020). Implications of COVID-19 for an ageing population. *The Medical Journal of Australia*, *213*(8), 342-344.

Hoyos, W., Aguilar, J., & Toro, M. (2023). Federated learning approaches for fuzzy cognitive maps to support clinical decision-making in dengue. E*ngineering Applications of Artificial Intelligence*, *123*, 106371. https://doi.org/10.1016/j.engappai.2023.106371.

Ieracitano, C., Mammone, N., Versaci, M., Varone, G., Ali, A.R., Armentano, A., Calabrese, G., Ferrarelli, A., Turano, L., Tebala, C., Hussain, Z., Sheikh, Z., Sheikh, A., Sceni, G., Hussain, A., & Morabito, F.C. (2022). A fuzzy-enhanced deep learning approach for early detection of Covid-19 pneumonia from portable chest X-ray images. *Neurocomputing*, *481*, 202-215.

Jaiswal, A.K., Tiwari, P., Kumar, S., Gupta, D., Khanna, A., & Rodrigues, J.J.P.C. (2019). Identifying pneumonia in chest X-rays: a deep learning approach. *Measurement*, *145*, 511-518.

Joshi, K., Tripathi, V., Bose, C., & Bhardwaj, C. (2020). Robust sports image classification using InceptionV3 and neural networks. *Procedia Computer Science*, *167*, 2374-2381.

Kafadar, A.H., Tekeli, G.G., Jones, K.A., Stephan, B., & Dening, T. (2022). Determinants for COVID-19 vaccine hesitancy in the general population: a systematic review of reviews. *Journal of Public Health*, *31*(11), 1829-1845.

Kandati, D.R., & Gadekallu, T.R. (2023). Federated learning approach for early detection of chest lesion caused by COVID-19 infection using particle swarm optimization. *Electronics*, *12*(3), 710. https://doi.org/10.3390/electronics12030710.

Kanwal, K., Khalid, S.G., Asif, M., Zafar, F., & Qurashi, A.G. (2024). Diagnosis of Community-Acquired pneumonia in children using photoplethysmography and Machine learning-based classifier. *Biomedical Signal Processing and Control*, *87*, 105367. https://doi.org/10.1016/j.bspc.2023.105367.

Kareem, A., Liu, H., & Velisavljevic, V. (2023). A federated learning framework for pneumonia image detection using distributed data. *Healthcare Analytics*, *4*, 100204. https://doi.org/10.1016/j.health.2023.100204.

Khan, S.H., & Alam, M.G.R. (2021). A federated learning approach to pneumonia detection. In *2021 International Conference on Engineering and Emerging Technologies* (pp. 1-6). IEEE. Istanbul, Turkey.

Kundu, R., Das, R., Geem, Z.W., Han, G.T., & Sarkar, R. (2021). Pneumonia detection in chest X-ray images using an ensemble of deep learning models. *PloS One*, *16*(9), e0256630. https://doi.org/10.1371/journal.pone.0256630.

Mabrouk, A., Díaz Redondo, R.P., Abd Elaziz, M., & Kayed, M. (2023). Ensemble federated learning: an approach for collaborative pneumonia diagnosis. *Applied Soft Computing*, *144*, 110500.

Makkar, A., & Santosh, K.C. (2023). SecureFed: federated learning empowered medical imaging technique to analyze lung abnormalities in chest X-rays. *International Journal of Machine Learning and Cybernetics, 14*, 2659-2670.

Malik, H., Naeem, A., Naqvi, R.A., & Loh, W.K. (2023). DMFL_net: a federated learning-based framework for the classification of COVID-19 from multiple chest diseases using X-rays. *Sensors* , *23*(2), 743.

Mooney, P. (2018). *Chest X-ray images (pneumonia)* [Dataset]. https://www.kaggle.com/datasets/paultimothymooney/chest-xray-pneumonia.

Nair, D.G., Nair, J.J., Reddy, K.J., & Narayana, C.V.A. (2022). A privacy preserving diagnostic collaboration framework for facial paralysis using federated learning. *Engineering Applications of Artificial Intelligence*, *116*, 105476. https://doi.org/10.1016/j.engappai.2022.105476.

Pan, Z., Wang, H., Wan, J., Zhang, L., Huang, J., & Shen, Y. (2024). Efficient federated learning for pediatric pneumonia on chest X-ray classification. *Scientific Reports*, *14*(1), 23272. https://doi.org/10.1038/s41598-024-74491-5.

Patel, P. (2020). *Chest X-ray (covid-19 & pneumonia)* [Dataset]. https://www.kaggle.com/datasets/prashant268/chest-xray-covid19-pneumonia.

Pneumonia. (n.d.). Retrieved February 20, 2024, from https://www.who.int/health-topics/pneumonia#tab=tab_1.

Prakash, A., Asswin, Kumar, D., Dora, A., Ravi, V., Sowmya, Gopalakrishnan, E.A., & Soman. (2023a). Transfer learning approach for pediatric pneumonia diagnosis using channel attention deep CNN architectures. *Engineering Applications of Artificial Intelligence*, *123*, 106416.

Prakash, J.A., Asswin, C.R., Ravi, V., Sowmya, V., & Soman, K.P. (2023c). Pediatric pneumonia diagnosis using stacked ensemble learning on multi-model deep CNN architectures. *Multimedia Tools and Applications*, *82*(14), 21311-21351.

Prakash, J.A., Ravi, V., Sowmya, V., & Soman, K.P. (2023b). Stacked ensemble learning based on deep convolutional neural networks for pediatric pneumonia diagnosis using chest X-ray images. *Neural Computing & Applications*, *35*(11), 8259-8279.

Rahimzadeh, M., & Attar, A. (2020). A modified deep convolutional neural network for detecting COVID-19 and pneumonia from chest X-ray images based on the concatenation of Xception and ResNet50V2. *Informatics in Medicine Unlocked*, *19*, 100360. https://doi.org/10.1016/j.imu.2020.100360.

Rehman, M.U., Shafique, A., Khan, K.H., Khalid, S., Alotaibi, A.A., Althobaiti, T., Ramzan, N., Ahmad, J., Shah, S. A., & Abbasi, Q.H. (2022). Novel privacy preserving non-invasive sensing-based diagnoses of pneumonia disease leveraging deep network model. *Sensors* , *22*(2), 461. https://doi.org/10.3390/s22020461.

Riedel, P., von Schwerin, R., Schaudt, D., Hafner, A., & Späte, C. (2023). ResNetFed: federated deep learning architecture for privacy-preserving pneumonia detection from COVID-19 chest radiographs. *International Journal of Healthcare Information Systems and Informatics: Official Publication of the Information Resources Management Association*, *7*(2), 203-224.

Sharma, S., & Guleria, K. (2025). A collaborative privacy preserved federated learning framework for pneumonia detection using diverse chest X-ray data silos. *International Journal of Mathematical, Engineering and Management Sciences*, *10*(2), 464-485.

Sharma, S., Guleria, K., & Dogra, A. (2025). FedPneu: federated learning for pneumonia detection across multiclient cross-silo healthcare datasets. *Current Medical Imaging*, *21*(2025), 1-41.

Sharma, S., Guleria, K., Kumar, S., & Tiwari, S. (2023). Deep learning based model for detection of vitiligo skin disease using pre-trained Inception V3. *International Journal of Mathematical, Engineering and Management Sciences*, *8*(5), 1024-1039.

Shiri, I., Salimi, Y., Sirjani, N., Razeghi, B., Bagherieh, S., Pakbin, M., Mansouri, Z., Hajianfar, G., Avval, A.H., Askari, D., Ghasemian, M., Sandoughdaran, S., Sohrabi, A., Sadati, E., Livani, S., Iranpour, P., Kolahi, S., Khosravi, B., Bijari, S., Zaidi, H. (2024). Differential privacy preserved federated learning for prognostic modeling in COVID-19 patients using large multi-institutional chest CT dataset. *Medical Physics*, *51*(7), 4736-4747. https://doi.org/10.1002/mp.16964.

Subashchandrabose, U., John, R., Anbazhagu, U.V., Venkatesan, V.K., & Ramakrishna, M.T. (2023). Ensemble federated learning approach for diagnostics of multi-order lung cancer. *Diagnostics (Basel, Switzerland)*, *13*(19), 3053. https://doi.org/10.3390/diagnostics13193053.

Wahab, H., Mehmood, I., Ugail, H., Ser, J.D., & Muhammad, K. (2023). Federated deep learning for wireless capsule endoscopy analysis: enabling collaboration across multiple data centers for robust learning of diverse pathologies. *Future Generations Computer Systems, 152,* 361-371. https://doi.org/10.1016/j.future.2023.10.007.

Wang, C., Chen, D., Hao, L., Liu, X., Zeng, Y., Chen, J., & Zhang, G. (2019). Pulmonary image classification based on inception-v3 transfer learning model. *IEEE Access: Practical Innovations, Open Solutions*, *7*, 146533-146541.

Zhang, R., Luo, W., Luo, Y., Zhang, H., & Wang, J. (2024). AFL-DCS: an asynchronous federated learning framework with dynamic client scheduling. *Engineering Applications of Artificial Intelligence*, *133*, 107927.